Hindawi Publishing Corporation
International Journal of Rotating Machinery
Volume 2012, Article ID 853767, 9 pages
doi:10.1155/2012/853767

Research Article

Some Improvements in a Gas Turbine Stator-Rotor Systems Core-Swirl Ratio Correlation

R. Da Soghe, B. Facchini, L. Innocenti, and M. Micio

Department of Energy "Sergio Stecco", University of Florence, 50139 Firenze, Italy

Correspondence should be addressed to R. Da Soghe, dasoghe@brun.de.unifi.it

Received 13 September 2011; Revised 3 March 2012; Accepted 8 March 2012

Academic Editor: Ting Wang

The present work concerns the turbulent flow inside a rotor-stator cavity with superimposed throughflow. The authors focused their analysis on a simple two-faced disk cavity, without shrouds, with interdisk-spacing sufficiently large so that the boundary layers developed on each disk are separated and the flow is turbulent. In such a system, the solid body rotation of the core predicted by Batchelor can develop. The evolution of the core-swirl ratio of the rotating fluid with an outward throughflow is studied by applying a classical experimental correlation, inserted in a one-dimensional (1D) in-house developed code. Results are compared to those predicted by CFD computations. Due to the discrepancies revealed, the authors provided a correction of the experimental correlation, based on CFD computation. Results thus obtained are finally in good agreement with CFD predictions.

1. Introduction

The turbulent flow inside rotating cavities has been investigated for some decades because of its relevance in turbomachinery design and application. Generally, cooler high-pressure purge air bled from the compressor is injected into the cavities with the aim of sealing them. Accomplishing the sealing of the cavity and the cooling of the metal, using the smallest possible amount of purge air, is a key objective in turbine design since the bleed-off of compressor air and its subsequent mixing with the main gas flow exact penalties on turbine performance.

First studies on the isothermal flow structure in rotating disk systems were performed at the beginning of the past century. The historical controversy created by Batchelor (1951) and Stewartson (1953) is well known [1]. The former specified the formation of a nonviscous core in the solid body rotation, confined between the two boundary layers which develop on the disks: the tangential velocity of the fluid can be zero everywhere apart from the rotor boundary layer. Later, Daily and Nece [2] noticed that the flow structure can be divided into four regimes, laminar and turbulent, with or without separated boundary layers.

With regarding rotor-stator systems with superimposed throughflow, some results have been published. Some authors [3] measured the average velocity profiles in the case of rotor-stator systems with a centrifugal imposed throughflow. Moreover, the authors showed that the flow parameter λ_{turb} is the similarity parameter of the turbulent flow that can be used directly to calculate the core-swirl ratio. Later on, Kurokawa and Toyokura [4] proposed a 1D model to calculate the core-swirl ratio and the pressure distribution within the cavity and introduced a coefficient of throughflow rate based on the rotating disk velocity. The authors validated the model by experimental measurements. In a subsequent paper [5], the same model was reviewed in order to allow its use for the rotating cavity with a narrow axial gap.

In another paper [6], the author solved the linear Ekman-layer equations for the case of a rotor-stator system with a superimposed radial outflow of fluid. The predicted rotational speed of the core between the boundary layers on the rotor and stator agrees well with published experimental measurements [3] when the superimposed flow rate is zero, but the theoretical solutions underestimate the core rotation when the flow rate is nonzero. Details concerning the solution of the turbulent momentum-integral equations for

the rotor to provide an approximation for the core rotation are also provided in the most comprehensive monograph on the state of understanding flow and heat transfer processes in rotating disk systems [1].

More recently, a certain number of papers devoted to the development and/or validation of analytical models for core-swirl ratio prediction are available in the literature. Among those, some papers are particularly interesting [7–11]. In these papers, the authors noticed that the equation that links β to the flow rate coefficient is according to a 5/7 power law profile.

In two of the above-cited papers [7, 8], the analytical law was validated by extensive pressure and velocity measurements, for different values of the interdisk gap and in a large range of Reynolds numbers and flow rates. The measurements are obtained in water for a turbulent Batchelor type of flow, by means of a laser Doppler anemometer. Experimental results performed at the same test rig in a wide range of Reynolds number and flow rate, in presence of inward and/or outward throughflow, were also used to validate an advanced second-order turbulence model [9–12]. The excellent agreement of numerical predictions with the velocity and pressure measurements confirmed that the described RSM turbulence model is a valuable tool for flow analysis in rotor-stator systems. Other authors focused their investigations on the application of standard turbulence models in solving swirled flow in rotating cavities [13–15]. In the first paper [13], the authors presented a CFD benchmark performed for closed cavity flow with rotor-stator, contrarotating, and corotating disks. The authors tested several turbulence models and compared numerical predictions with measurements of an experimental test case: k-ω shear-stress transport SST model demonstrated the best concordance. In another paper [14], the authors focused their works on the comparison of CFD predictions obtained with a two-equation k-ω SST turbulence model with experimental measurements carried out by hot-wire anemometry and three-holes pressure probes. The authors reveal that the experiments are qualitatively well described by numerical results. Also in the last cited paper [15], the authors performed a CFD campaign by simulating the turbulence with the k-ω SST model. This selection was based on a survey of turbulence models in two-dimensional, axisymmetric CFD analyses for a shrouded rotor-stator cavity with the disk walls at different speeds. In comparison to measured velocity profiles, the k-ω SST model demonstrated the best overall agreement.

The present study is focused on the turbulent flow inside a rotor-stator cavity with superimposed centrifugal throughflow. The analysis is limited to a simple two-faced disk cavity, without shrouds, with an axial gap so large that a core region sets in. The distribution of the core-swirl ratio of the rotating fluid and its pressure rise are predicted by applying the experimental correlation proposed by Daily et al. [3] inserted in the 1D in-house code. CFD predictions led the authors to review the correlation in order to minimize the revealed discrepancies. Finally, the criterion to determine the transition from Batchelor to Stewartson types of flow is also gained from this study.

2. 1D In-House Code Modeling

A detailed description of the in-house code can be found in two previously published papers [16, 17] together with the discussion of the results obtained in a preliminary code testing campaign. Those results show that the 1D code is able to provide fairly accurate predictions about fluid-dynamics quantities trends, but it was also pointed out that the program shows some discrepancies, with respect to 3D CFD data, in terms of core-swirl ratio prediction. Those discrepancies, in principle, could be addressed both to the correlations used to evaluate the disk friction coefficients and to the mass flow rate pumped by the rotor disk. On the other hand, an accurate and reliable core-swirl ratio prediction plays a fundamental role in the rotor-stator system analysis.

In the present work, the authors performed an exhaustive and detailed study using the following experimental correlation proposed by Daily et al. [3]:

$$\frac{\beta}{\beta^*} = \left(12.74 \cdot \lambda_{\text{turb}} x^{-13/5} + 1\right)^{-1}. \quad (1)$$

It links the swirl-core ratio β to the turbulent flow parameter λ_{turb} and was derived from the experimental measurements of El-Oun and Pincombe and from the numerical predictions of Vaughan [1, 6]. That correlation evaluates $\beta/\beta^* = 1$ for $\lambda_{\text{turb}} = 0$, β^* being the core-swirl ratio in absence of throughflow: in the present work $\beta^* = 0.426$ [3].

Figure 1 shows the above-cited data compared with the correlation trend. It is clearly evident that for $\lambda_{\text{turb}} x^{-13/5} = 0.22$, the value of the core rotation rate is different from zero, while the "improved approximation" proposed by Owen and Rogers [2] predicts that for a higher value of the flow parameter, a Stewartson flow type must set in. This means that the mass flow rate entrained by the boundary layer on the rotor is underestimated, and the core rotation must start for a higher value of $\lambda_{\text{turb}} x^{-13/5}$.

In the following sections, the authors present a correction to improve the agreement of the correlation results with the experimental and numerical data. Moreover, a different value of $\lambda_{\text{turb}} x^{-13/5}$ that determines the transition from the Stewartson to the Batchelor flow type is defined from the CFD predictions.

3. Tested Geometry and Simulations Conditions

The analyzed geometry consists in a simple-plane-faced disk rotor-stator cavity. The cavity dimensions are quoted in Table 1(a). The gap ratio G value was selected in order to assure that separate boundary layers exist (region IV). In the present study, the nondimensional flow parameters range (Table 1(b)) was chosen in order to perform the numerical campaign within the typical gas turbine operation field. Six values for the λ_{turb} and five for the C_w parameters were chosen, for a total of 30 runs. The selected range enabled the development of a core region within the wheel space region, in order to perform a detailed evaluation of 1D program capabilities in predicting the growth of a recirculation. All simulations were performed in adiabatic conditions in order to avoid superpositions of heat transfer. The numerical tests

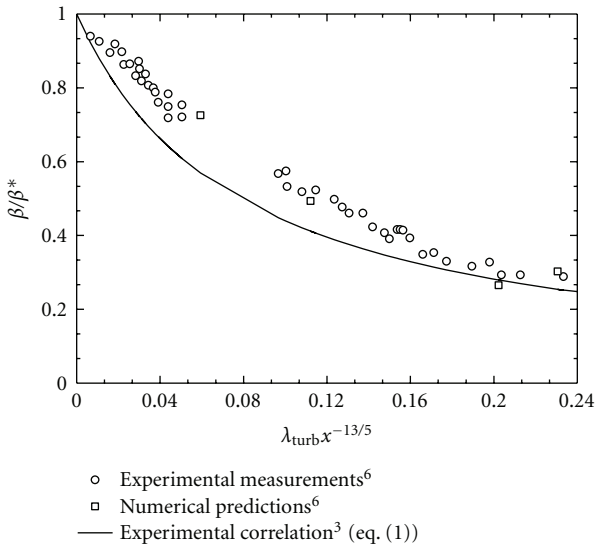

Figure 1: β/β^* versus $\lambda_{\text{turb}}x^{-13/5}$.

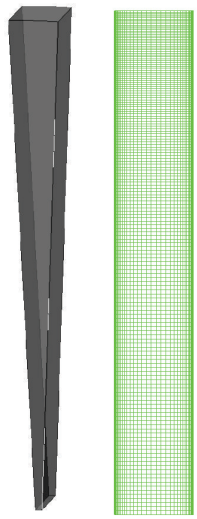

Figure 2: The 5° sector model for CFD simulation.

were conducted in a quiescent environment, and thus no blades and vanes were modeled.

4. CFD Computations

CFD steady-state calculations were performed with the commercial 3D Navier-Stokes solver CFX-10.0. All numerical simulations were performed with 5° sector model (Figure 2). As already discussed, the numerical analysis here reported is focused on the inner cavity flow, so the flowpath was not included in the computations. Periodicity was imposed at the sectors circumferential boundaries, while no-slip and adiabatic conditions were applied on solid surfaces. The pressure boundary condition was imposed at the outlets, while mass flow rates were imposed at the inlets.

Table 1

(a)

b/r_{in}	7.50
G	0.13

(b)

C_w	$7\cdot10^3 \div 2\cdot10^4$
λ_{turb}	0.09 ÷ 0.2

Compressibility effects were taken into account, and high-resolution advection schemes were used. This advection scheme enforces a boundedness criterion throughout the domain. In flow regions with low variable gradients, the scheme consists in a second-order advection scheme. In areas where the gradients change sharply, the model switches to an upwind scheme to prevent overshoots and undershoots and maintain robustness.

The fluid was modeled as ideal gas, and the properties of specific heat capacity, thermal conductivity, and viscosity were assumed as a function of temperature. Energy equation was solved in terms of total temperature, and viscous heating effects were accounted for. The k-ω SST turbulence model, in its formulation kept available by the CFD solver, was used in conjunction with a low Reynolds approach. The choice of the turbulence model is related to the evidence provided by Wu et al. Debuchy et al., and Roy et al. [13–15]. Furthermore, recently, Da Soghe et al. [18] have done an extensive study to point out if the k-ω SST turbulence model (and more in general the RANS approach) permits to confidently catch the fluid flow within stator-rotor cavities like those analyzed in this work. The main finding of the work is that the SST model is in good agreement with the experimental data for both the mean and turbulent fields in a wide range of operating conditions.

The mesh generation tool ICEM CFD was used to generate a hexahedral cells mesh. A number of grid sensitivity tests were conducted in order to ensure mesh independence solutions. The final mesh dimension, in terms of elements number, is around 60 k elements (Figure 2). The convergence of solutions was assessed by monitoring the torque on the cavities walls, mass flow through the outlet, and residuals.

5. CFD Results

A first validation of CFD computations was performed by comparing our numerical predictions with the published experimental and numerical data [6]. As shown in Figure 3, the agreement within the common range, in terms of core-swirl ratio versus the local flow rate coefficient $\lambda_{\text{turb}}x^{-13/5}$, is good. Moreover, within the chosen nondimensional flow parameters range (Table 1(b)), all CFD calculations predicted quite similar flow fields.

As an example, Figure 4 shows the distribution of β/β^* and $v_r/(\Omega \cdot r)$ obtained for $C_w = 16730$ and $\lambda_{\text{turb}} = 0.09$. It is clearly evident that at the inlet of the cavity the tangential velocity of the fluid is zero everywhere apart from the rotor

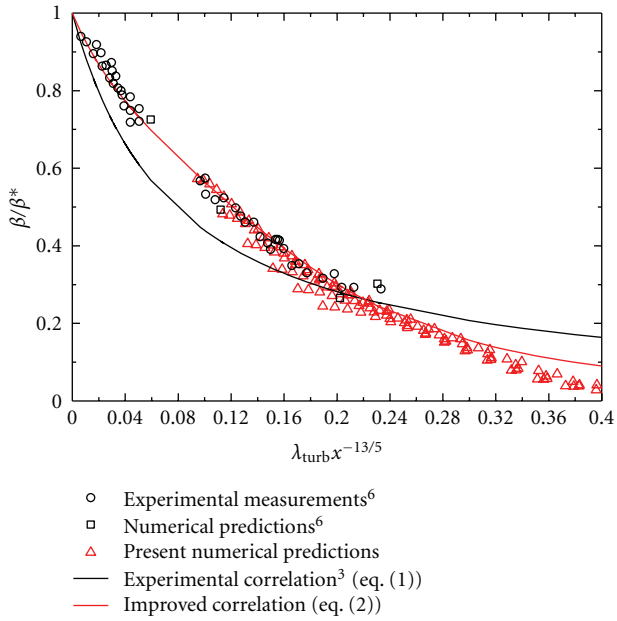

FIGURE 3: β/β^* versus $\lambda_{turb}x^{-13/5}$: present numerical predictions and improved correlation.

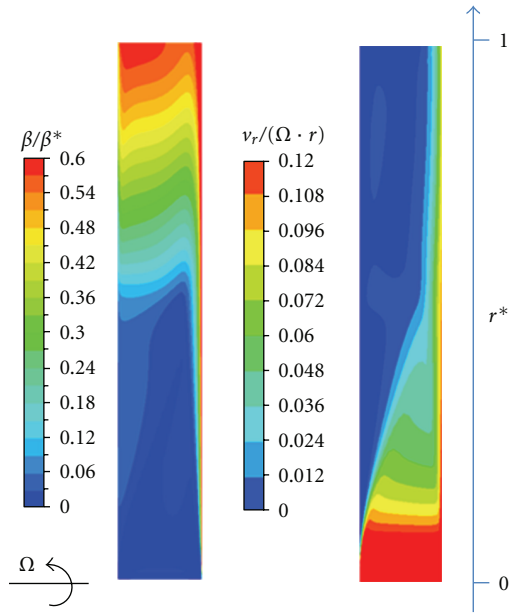

FIGURE 4: CFD results: β/β^* and $v_r/(\Omega \cdot r)$ distribution (C_w = 16730, λ_{turb} = 0.09).

boundary layer and the centrifugal throughflow which fills the whole axial gap between the disks. On the contrary, in the upper region of the calculation domain, a rotating core confined between the two boundary layers develops.

The two flow structures described above are separated by a transition region that, in this case, fills a wide portion of the cavity. Starting from the entry of the calculation domain, that region is characterized by a sharp reduction of the radial

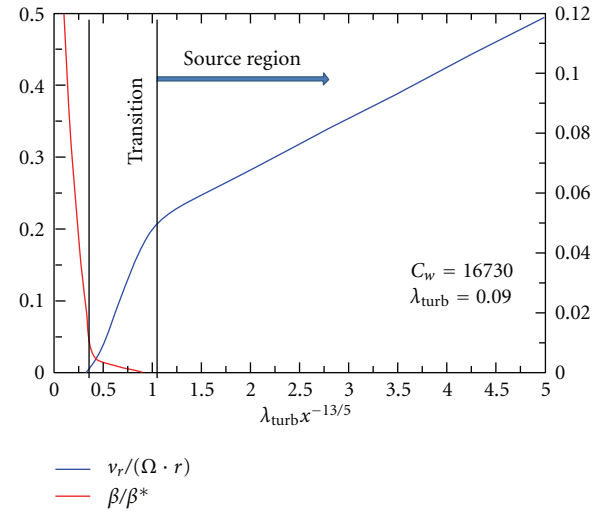

FIGURE 5: Nondimensional radial and tangential velocity (mass flow averaged on constant radius surfaces).

velocity component and by a slight rise of the circumferential one (Figure 5).

The Stewartson flow type can be recognized by the absence of the rotating core, while the Batchelor flow structure is revealed by the strong increase of β/β^*. In the whole computation domain, the radial velocity component behaves inversely to the circumferential one (Figure 5). Concerning the radial localization of the transition region, it can define the beginning of the core region approximately from $\lambda_{turb}x^{-13/5} = 0.4$ (Figure 5) for the whole of the CFD runs. The last statement is confirmed by Figures 6 and 7. In these figures, the dotted line represents the cavity outflow mass flow rate that exceeds the superimposed one.

To point out the mentioned profile, this parameter was evaluated on a number of constant radius isosurfaces accordingly with the following expression:

$$\dot{m}_{out,r} = \frac{1}{2}\left(\int_{A,r} p\|v_r\|dA - \dot{m}_{sup}\right), \quad (2)$$

where A, r represents the generic isosurface at constant radius. Referring to Figure 6, the increase of the $\dot{m}_{out,r}$ parameter at the lower radii can be motivated by the presence of the inner vortex shown in Figure 8.

After that vortex, $\dot{m}_{out,r}$ falls down close to zero and then takes off as the core region sets in. As shown by Figure 7, the $\dot{m}_{out,r}$ profile takes off (i.e., the core region starts), for $\lambda_{turb}x^{-13/5}$ higher than 0.22 meaning that CFD predicts a higher rotor disc pumped mass flow rate with respect of the "improved approximation" proposed by Owen and Rogers [2]. These evidences are true for all tested conditions reported in this paper.

5.1. Improved Correlation. In order to improve the agreement of the correlation inserted in the 1D program [3] equation (1) with the published results [6] and present CFD computations (Figure 3), the authors defined a corrective

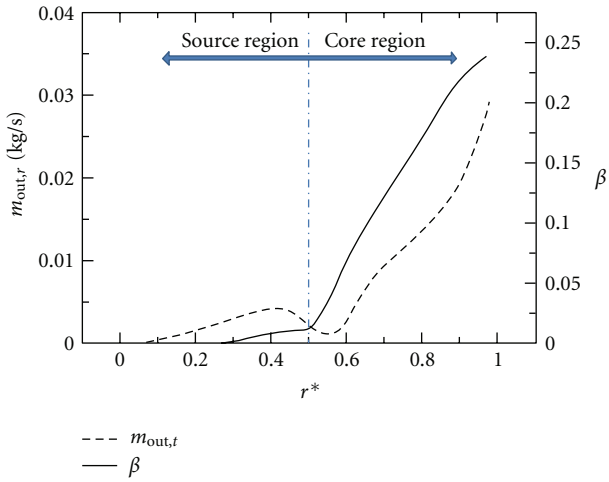

FIGURE 6: $\dot{m}_{out,r}$ and β over radius.

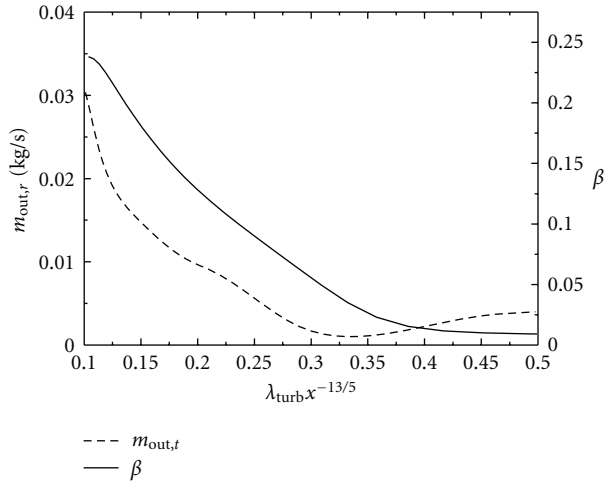

FIGURE 7: $\dot{m}_{out,r}$ and β over $\lambda_{turb}x^{-13/5}$.

function that has to be applied to the core-swirl ratio calculated by means of correlation equation (1),

$$\beta_{imp} = K \cdot \beta. \tag{3}$$

Starting from the data plotted in Figure 3, the authors found that the most suitable form for the multiplicative function K is the following:

$$K = \left[-23.5\left(\lambda_{turb}x^{-13/5}\right)^3 + 26.0\left(\lambda_{turb}x^{-13/5}\right)^2 - 4.6\left(\lambda_{turb}x^{-13/5}\right) + 1\right]^{-1}. \tag{4}$$

The improved correlation defined from (3) reduces the average error from 14% to 3.8% with respect to both numerical and experimental data. It allows to estimate accurately the core-swirl ratio in a wide range value of $\lambda_{turb}x^{-13/5}$ (Figure 3). Moreover, when a rotating core takes place, that is, for the lowest values of the local flow rate coefficient, the improved correlation predicts core-swirl ratios higher than

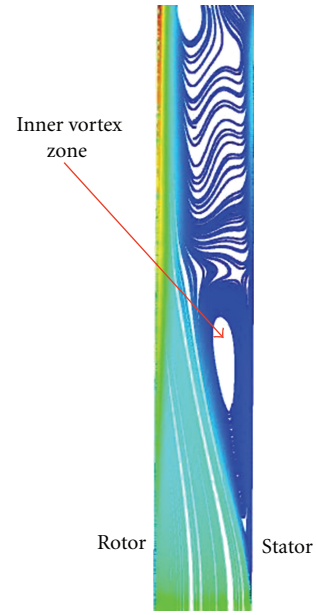

FIGURE 8: Inner vortex location.

the correlation (1). On the contrary, for $\lambda_{turb}x^{-13/5} > 0.22$, the application of the multiplicative function K leads to lower values of β, if compared with the correlation of Daily et al. [3] (Figure 3).

6. 1D Program Results

The 1D in-house program has been tested in detail, under the same calculation conditions as in the CFD analysis. In order to appropriately compare its predictions with the 3D calculations, the authors chose as reference parameter the local pressure coefficient $C_p(r)$, defined in the following equation:

$$C_p(r) = \frac{p(r) - p_{out}}{(1/2)\rho(\Omega b)^2}. \tag{5}$$

That parameter is closely related to the core-swirl ratio as the pressure rise can be expressed with the following equation:

$$\frac{1}{\rho} \cdot \frac{dp}{dr} = r \cdot (\Omega\beta)^2 - v_r \cdot \frac{dv_r}{dr}. \tag{6}$$

Then, the comparison in terms of local pressure coefficient appears to be particularly suitable to verify the accuracy of the correlations inserted into the 1D program.

Figures 9 and 10 show, respectively, the local pressure coefficient versus the radial span predicted by CFD computations and by the 1D program, using the correlation equation (1) with or without the correction. In particular, in Figure 9 results concerning six different λ_{turb} values for the same nondimensional mass flow rate are plotted. The authors want to stress that the correction proposed improves the agreement of 1D predictions with CFD computation, in terms both of local pressure distribution and global pumping. The results shown in Figure 10, concerning the

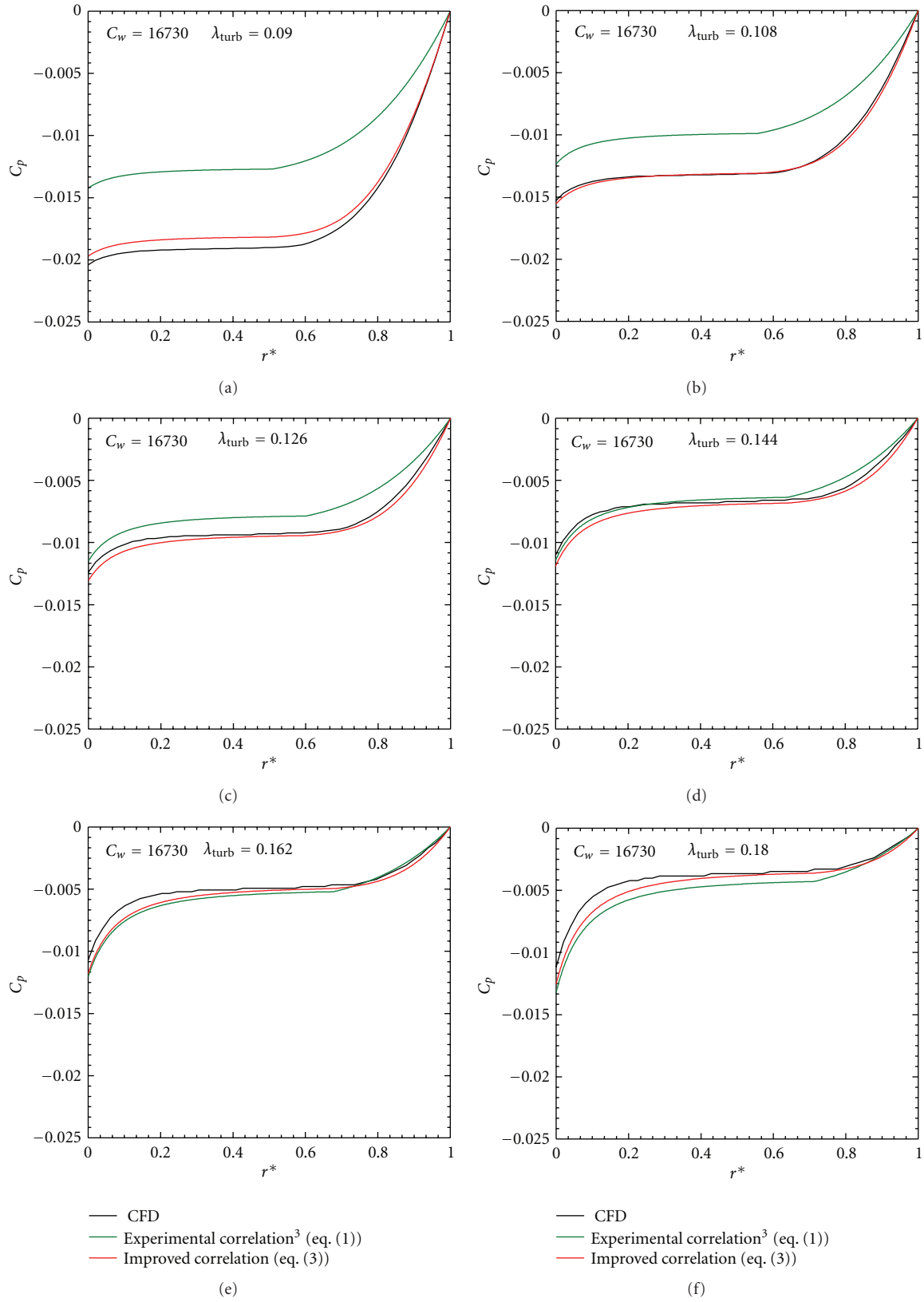

Figure 9: Local pressure coefficient versus radial span (C_w = 16730, λ_{turb} = 0.09 ÷ 0.180).

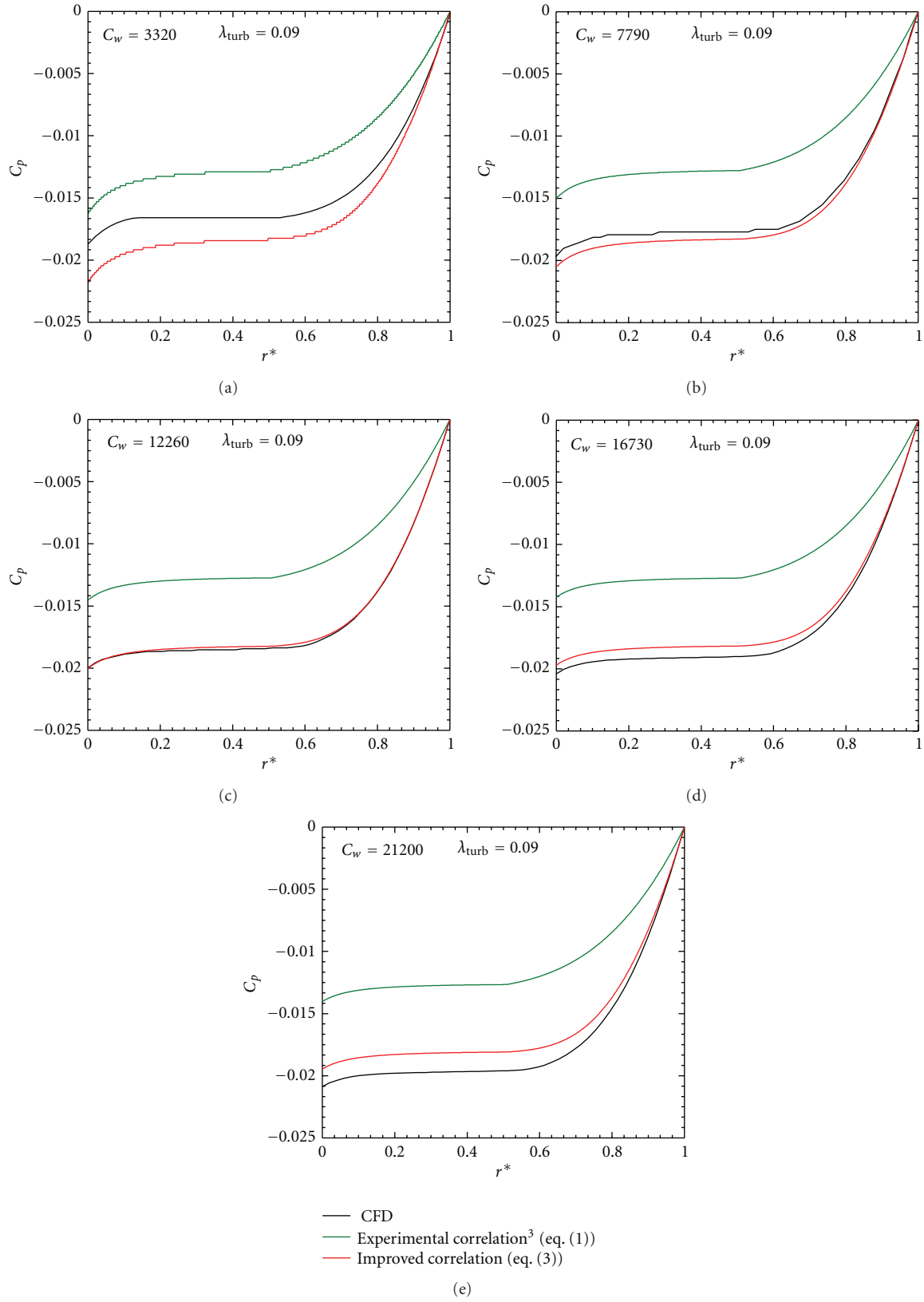

Figure 10: Local pressure coefficient versus radial span ($C_w = 3320 \div 21200$, $\lambda_{turb} = 0.09$).

six different nondimensional flow rates for the same value of λ_{turb}, confirm what the authors noticed above.

For all the cases analyzed, it is possible to recognize a Stewartson flow type at the lower radius, where the diffusive effect is dominant due to the increase of the cross-section (heavier near the inlet of the cavity) and a Batchelor flow type where the pressure rises greatly due to the increase of the tangential velocity.

6.1. Effect of the Turbulent Flow Parameter. The increase of the turbulent flow parameter for a given nondimensional flow rate (Figure 9) reduces the radial extension of the Batchelor flow region. Evidence of this effect is the shift towards higher radial span values of the significant pressure rise. That phenomenon, already known in the literature [1, 7–11], causes a reduction of the global cavity pumping. As the improved correlation acts in the core region, in case of high turbulent, flow discrepancies between the original approach and the improved one are limited. Finally, it should be pointed out how the rise of the λ_{turb} parameter for a given C_w coincides with a rotational Reynolds number decrease.

6.2. Effect of the Nondimensional Flow Rate. The increase of the nondimensional flow rate for a given turbulent flow parameter (Figure 10) does not modify the flow field significantly that develops into the cavity. Particularly, the radial extension of the Batchelor flow type region remains unchanged as the whole pressure rises. It is in fact well known that the pumping magnitude only depends on the turbulent flow parameter [1].

7. Conclusions

Computational fluid dynamics is a powerful tool capable of providing useful information in understanding the phenomena that are involved in cavity design. However during predesign and test phases, more simplified calculation tools are profitably used, as they provide very important suggestions for designers. For this purpose, the authors, modeling the wheel space cavities on a macroscopic basis, developed a simplified calculation tool. The in-house one-dimensional code estimates the shape of the radial profile of pressure in reasonably good agreement with CFD predictions [17] but provides unreliable evaluation of the overall pressure growth. This effect was addressed to the β values appreciated by the use of the Daily et al. correlation [3]. CFD predictions led the authors to review that correlation through a suitable correction term in order to minimize the revealed discrepancies.

The mentioned term was found as a third-degree polynomial expression of $\lambda_{\text{turb}} x^{-13/5}$, and its usage reduces the average error from 14% to 3.8% with respect to CFD and experimental data. The transition from the Stewartson to the Batchelor flow type was also investigated as the experimental and numerical results show that the "improved approximation" proposed by Owen and Rogers [1] seems to give unreliable prediction.

Considering the mentioned improvements, the in-house one-dimensional code predictions are in good agreement with CFD data.

Nomenclatures

b: Outer radius of disk [m]
C_p: Local pressure coefficient [−]
C_w: Nondimensional flow rate $\text{m}/(\mu b)$ [−]
G: Gap ratio s/b [−]
K: Multiplicative function [−]
$\dot{m}$: Mass flow rate [kg/s]
p: Pressure [Pa]
r: Radius [m]
r^*: Radial span $(r - r_{\text{in}})/(b - r_{\text{in}})$ [−]
Re_ϕ: Rotational Reynolds number $(p \cdot \Omega \cdot b^2)/\mu$ [−]
s: Cavity axial gap [m]
v_r: Radial velocity [m/s]
v_t: Tangential velocity [m/s]
x: Nondimensional radius r/b [−].

Greeks

β: Core-swirl ratio ω/Ω [−]
λ_{turb}: Turbulent flow parameter $C_w/\text{Re}_\phi^{4/5}$ [−]
μ: Dynamic viscosity [Pa · s]
ρ: Density [kg/m^3]
ω: Angular speed of the rotating core [rad/s]
Ω: Angular speed of rotating disk [rad/s].

Subscripts

in: Inner, referred to the cavity
out: Outer, referred to the cavity
imp: Improved value
sup: Superimposed.

References

[1] J. M. Owen and R. H. Rogers, *Flow and Heat Transfer in Rotating-Disc Systems - Vol.1: Rotor-Stator Systems*, W. D. Morris, Ed., John Wiley & Sons, New York, NY, USA, 1989.

[2] J. W. Daily and R. E. Nece, "Chamber dimension effects on induced flow and frictional resistance of enclosed rotating disks," *Journal of Basic Engineering*, vol. 82, pp. 217–232, 1960.

[3] J. W. Daily, W. D. Ernst, and V. V. Asbedian, *Enclosed Rotating Disks with Superposed Throughflow, Report no. 64*, M.I.T., Department of Civil Engineering, 1964.

[4] J. Kurokawa and T. Toyokura, "Study on axial thrust of radial flow turbomachinery," in *Proceedings of the 2nd International JSME Symposium Fluid Machinery and Fluid Mechanics*, Tokyo, Japan, 1972.

[5] J. Kurokawa and M. Sakuma, "Flow in a narrow gap along an enclosed rotating disk with through-flow," *JSME International Journal Series B*, vol. 31, no. 2, pp. 243–251, 1988.

[6] J. M. Owen, "Approximate solution for the flow between a rotating and a stationary disk," *Journal of Turbomachinery*, vol. 111, no. 3, pp. 323–332, 1989.

[7] S. Poncet, M. P. Chauve, and P. Le Gal, "Turbulent rotating disk flow with inward throughflow," *Journal of Fluid Mechanics*, vol. 522, pp. 253–262, 2005.

[8] S. Poncet, M.-P. Chauve, and P. Le Gal, "Study of the entrainment coefficient of the fluid in a rotor-stator cavity," in *Proceedings of the 6th European Conference on Turbomachinery-Fluid Dynamics and Thermodynamics*, G. Bois, C. Sierverding, M. Manna, and T. Arts, Eds., vol. 1, pp. 246–256, 2005.

[9] S. Poncet, R. Schiestel, and M. P. Chauve, "Centrifugal flow in a rotor-stator cavity," *Journal of Fluids Engineering, Transactions of the ASME*, vol. 127, no. 4, pp. 787–794, 2005.

[10] S. Poncet, R. Schiestel, and M.-P. Chauve, "Turbulence modelling and measurements in a rotor-stator system with throughflow," in *Engineering Turbulence Modelling and Experiments 6*, W. Rodi and M. Mulas, Eds., pp. 761–770, Elsevier, New York, NY, USA, 2005.

[11] S. Poncet, M. P. Chauve, and R. Schiestel, "Batchelor versus Stewartson flow structures in a rotor-stator cavity with throughflow," *Physics of Fluids*, vol. 17, no. 7, pp. 1–15, 2005.

[12] R. Debuchy, S. Poncet, F. Abdel Nour, and G. Bois, "Experimental and numerical investigation of turbulent air flow behaviour in a rotor-stator cavity," in *Proceedings of the European Turbomachinery Conference*, 2009.

[13] C. Wu, K. McCusker, B. Vaisman, and R. Paolillo, "CFD analysis prediction of heat transfer coefficient in rotating cavities with radial outflow," in *51st ASME Turbo Expo*, pp. 1515–1525, May 2006.

[14] R. Debuchy, S. Della Gatta, E. D'Haudt, G. Bois, and F. Martelli, "Influence of external geometrical modifications on the flow behaviour of a rotor-stator system: numerical and experimental investigation," *Proceedings of the Institution of Mechanical Engineers A*, vol. 221, no. 6, pp. 857–864, 2007.

[15] R. P. Roy, D. W. Zhou, S. Ganesan, C. Z. Wang, R. E. Paolillo, and B. V. Johnson, "The flow field and main gas ingestion in a rotor-stator cavity," ASME Paper GT2007 27671, 2007.

[16] C. Bianchini, R. Da Soghe, B. Facchini et al., "Development of numerical tools for stator-rotor cavities calculation in heavy-duty gas turbines," in *ASME Turbo Expo*, pp. 1667–1679, June 2008.

[17] L. Innocenti, M. Micio, R. Da Soghe, and B. Facchini, "Analysis of Gas Turbine Rotating Cavities by an One Dimensional Model," ISROMAC Paper(12-2008-20161), 2008.

[18] R. Da Soghe, L. Innocenti, A. Andreini, and S. Poncet, "Numerical benchmark of turbulence modeling in gas turbine rotor-stator system," GT2010-22627.